



Publication Year	2020
Acceptance in OA	2022-02-23T12:16:33Z
Title	Latest results of dark matter detection with the DarkSide experiment
Authors	Picciau E., Agnes P., Albuquerque I.F.M., Alton A.K., Ave M., Back H.O., Batignani G., Biery K., Bocci V., Bonfini G., Bonivento W.M., Bottino B., Bussino S., Cadeddu M., Cadoni M., Calaprice F., Caminata A., Canci N., Candela A., Caravati M., Cariello M., Carlini M., Carpinelli M., Catalanotti S., Cataudella V., Cavalcante P., CAVUOTI, STEFANO, Chepurnov A., Cicalò C., Cocco A.G., Covone G., D'Angelo D., Davini S., de Candia A., de Cecco S., de Deo M., de Filippis G., DE ROSA, G., Derbin A.V., Devoto A., Di Eusanio F., D'Incecco M., Di Pietro G., Dionisi C., Downing M., D'Urso D., Edkins E., Empl A., Fiorillo G., Fomenko K., Franco D., Gabriele F., Galbiati C., Ghiano C., Giagu S., Giganti C., Giovanetti G.K., Gorchakov O., Goretti A.M., Granato F., Grobov A., Gromov M., Guan M., Guardincerri Y., Gulino M., Hackett B.R., Herner K., Hossein B., Hughes D., Humble P., Hungerford E.V., Ianni A., Ippolito V., Johnson T.N., Keeter K., Kendziora C.L., Kochanek I., Koh G., Korabelv D., Korga G., Kubankin A., Kuss M., la Commara M., Lai M., Li X., Lissia M., Longo G., Machado A.A., Machulin I.N., Mandarano A., Mapelli L., Mari S.M., Maricic J., Martoff C.J., Messina A., Meyers P.D., Milincic R., Monte A., Morrocchi M.
Publisher's version (DOI)	10.1393/ncc/i2020-20026-3
Handle	http://hdl.handle.net/20.500.12386/31450
Journal	IL NUOVO CIMENTO C
Volume	43

Latest results of dark matter detection with the DarkSide experiment

E. PICCIAU^(*)

*INFN, Sezione di Cagliari and Dipartimento di Fisica, Università degli Studi di Cagliari
Cagliari, Italy*

received 8 June 2020

Summary. — In this contribution the latest results of dark matter direct detection obtained by the DarkSide Collaboration are discussed. New limits on the scattering cross-section between dark matter particles and baryonic matter have been set. The results have been reached using the DarkSide-50 detector, a double-phase Time Projection Chamber (TPC) filled with ^{40}Ar and installed at Laboratori Nazionali del Gran Sasso (LNGS). In 2018, the DarkSide Collaboration has performed three different types of analysis. The so-called high-mass analysis into the range between $\sim 10\text{ GeV}$ and $\sim 1000\text{ GeV}$ is discussed under the hypothesis of scattering between

^(*) On behalf of P. Agnes, I. F. M. Albuquerque, A. K. Alton, M. Ave, H. O. Back, G. Batignani, K. Biery, V. Bocci, G. Bonfini, W. M. Bonivento, B. Bottino, S. Bussino, M. Cadeddu, M. Cadoni, F. Calaprice, A. Caminata, N. Canci, A. Candela, M. Caravati, M. Cariello, M. Carlini, M. Carpinelli, S. Catalanotti, V. Cataudella, P. Cavalcante, S. Cavuoti, A. Chepurinov, C. Cicalò, A. G. Cocco, G. Covone, D. D'Angelo, S. Davini, A. De Candia, S. De Cecco, M. De Deo, G. De Filippis, G. De Rosa, A. V. Derbin, A. Devoto, F. Di Eusanio, M. D'Incecco, G. Di Pietro, C. Dionisi, M. Downing, D. D'Urso, E. Edkins, A. Empl, G. Fiorillo, K. Fomenko, D. Franco, F. Gabriele, C. Galbiati, C. Ghiano, S. Giagu, C. Giganti, G. K. Giovanetti, O. Gorchakov, A. M. Goretti, F. Granato, A. Grobov, M. Gromov, M. Guan, Y. Guardincerri, M. Gulino, B. R. Hackett, K. Herner, B. Hosseini, D. Hughes, P. Humble, E. V. Hungerford, Al. Ianni, An. Ianni, V. Ippolito, T. N. Johnson, K. Keeter, C. L. Kendziora, I. Kochanek, G. Koh, D. Korablev, G. Korga, A. Kubankin, M. Kuss, M. La Commara, M. Lai, X. Li, M. Lissia, G. Longo, A. A. Machado, I. N. Machulin, A. Mandarano, L. Mapelli, S. M. Mari, J. Maricic, C. J. Martoff, A. Messina, P. D. Meyers, R. Milincic, A. Monte, M. Morrocchi, V. N. Muratova, P. Musico, A. Navrer Agasson, A. O. Nozdrina, A. Oleinik, M. Orsini, F. Ortica, L. Pagani, M. Pallavicini, L. Pandola, E. Pantic, E. Paoloni, K. Pelczar, N. Pelliccia, E. Picciau, A. Pocar, S. Pordes, S. S. Poudel, H. Qian, F. Ragusa, M. Razeti, A. Razeto, A. L. Renshaw, M. Rescigno, Q. Riffard, A. Romani, B. Rossi, N. Rossi, D. Sablone, O. Samoylov, W. Sands, C. Savarese, B. Schlitzer, E. Segreto, D. A. Semenov, A. Shchagin, A. Sheshukov, P. N. Singh, M. D. Skorokhvatov, O. Smirnov, A. Sotnikov, C. Stanford, S. Stracka, Y. Suvorov, R. Tartaglia, G. Testera, A. Tonazzo, P. Trinchese, E. V. Unzhakov, M. Verducci, A. Vishneva, R. B. Vogelaar, M. Wada, T. J. Waldrop, H. Wang, Y. Wang, A. W. Watson, S. Westerdale, M. M. Wojcik, X. Xiang, X. Xiao, C. Yang, Z. Ye, C. Zhu and G. Zuzel.

dark matter and Ar nuclei. The low-mass analysis, performed using the same hypothesis, extends the limit down to ~ 1.8 GeV. Through a different hypothesis, that predicts dark matter scattering off the electrons inside of the Ar atom, it has been possible to set limits for sub-GeV dark matter masses.

1. – Introduction

A good deal of past and recent astrophysical and cosmological evidence has indicated that the visible matter that makes up stars, galaxies and other objects that we have so far detected is only a small fraction of the mass which makes up the Universe. The unknown matter is named as dark matter, which is unseen by direct methods but whose presence is detected by studying the evolution of the galaxies themselves as revealed, for example, by measuring their rotation as a function of distance from the center. Looking for direct evidence of dark matter has been underway for many years, but so far no signal has been observed. Most of these studies have involved a search for Weakly Interacting Massive Particles (WIMPs), whose presence would be indicated by the detection of a recoiling nucleus in a large volume detector. Among direct detection techniques, dual-phase TPCs filled up with liquified noble gases such as argon or xenon are the most promising for masses larger than few GeV. They allow to obtain large, homogeneous, low-background, and self-shielding detectors. In particular, the usage of Liquid Argon (LAr) guarantees an excellent discrimination power ($>10^8$) in the scintillation pulse shape between nuclear and electron recoils. However, a disadvantage of natural argon is that it contains an amount of cosmogenic ^{39}Ar , whose β^- decays contribute in contamination inside of the detector. This problem has been reduced using Underground Argon (UAr), in which the amount of ^{39}Ar is 3 order of magnitude less. One of the current LAr detectors is DarkSide-50, located at Laboratori Nazionali del Gran Sasso (LNGS) and it consists of a double-phase LAr TPC with an active mass of (46.4 ± 0.7) kg of low-radioactivity argon deployed in a Liquid-Scintillator Veto (LSV) and a Water Cherenkov Veto (WCV). In this paper, the latest results of DarkSide-50 obtained using data accumulated in 532.4 live-days, from August 2015 to October 2017, are shown and discussed.

2. – The DarkSide-50 detector

The DarkSide-50 apparatus [1] is composed of three nested detectors (see fig. 1). The outermost is the WCD, a cylinder tank used to shield and to perform anti-coincidence to reject events caused by residual fluxes of cosmic muons. The WCD is an 11 m-diameter, 10 m high cylindrical tank filled with high-purity water. More internally there is the LSV, that is a 4 m diameter stainless-steel sphere filled up with 30 tons of liquid scintillator [2]. LSV serves as a shield and is useful to discriminate radiogenic and cosmogenic neutrons, γ -rays and cosmic muons. At the center of the LSV there is the DarkSide-50 TPC, which is the effective dark matter detector. Inside of that, LAr is maintained at a temperature of $T \sim 85$ K using an external circulation loop connected with the cryostat, while the gas passes out of the detector system to the cryogenic purification system, located on the top of the water tank, in the radon-suppressed clean room, which contains all equipment interfacing directly with the detectors. The detector system is located in Hall C of LNGS

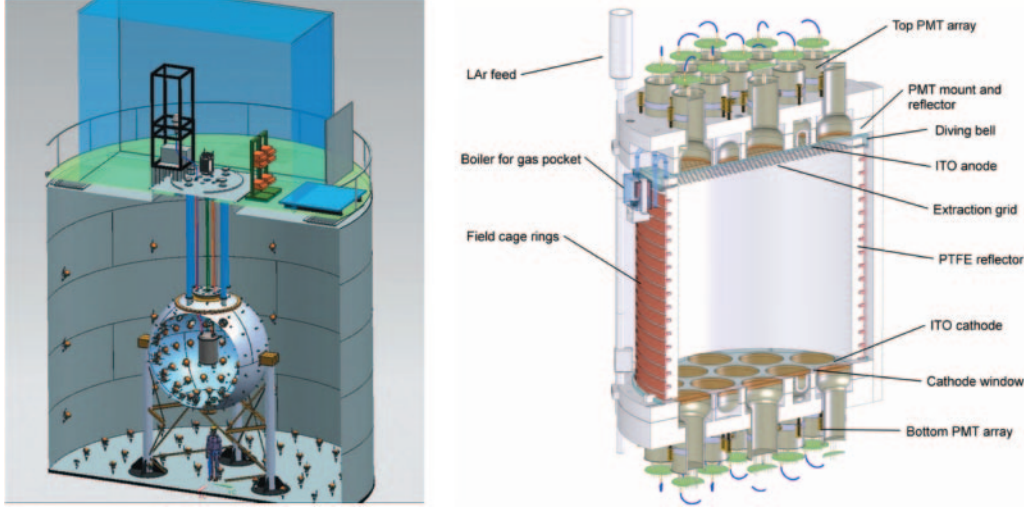


Fig. 1. – DarkSide-50 detector apparatus. On the left, the water tank WCD, the LSV sphere and the liquid argon TPC are shown. On the right a more detailed view of the TPC is presented.

at a depth of 3800 m.w.e. (meter water equivalent). The working principle of DarkSide-50 is based on the signals produced when the argon recoils. In the LAr phase, the recoil produces a scintillation signal named S1. In addition to this, ionisation electrons are produced and carried towards the upper part of the TPC thanks to an electric field of 200 V/cm. Part of this energy is released in form of phonons and is not detected. Once electrons reach the gas phase, a second signal, called electroluminescence signal or S2, is produced. Two arrays of 19 PMTs at the top and the bottom of the TPC collect the light. The maximum drift time, corresponding to the height of the TPC (35.6 cm), is $375 \mu\text{s}$. From the time delay between S1 and S2 it is possible to obtain the z -position of the particle interaction. The spatial resolution is estimated to be 0.6 cm. Both signals, S1 and S2, are measured by the same PMT array. This allows to exploit a three-dimensional position of the energy deposition. This helps to reject surface backgrounds and multi-sited events. A LAr detector has the possibility to exploit the technique of Pulse Shape Discrimination (PSD) that allows to identify whether a signal is due to an Electron Recoil (ER) process, such as β 's or γ 's, or to a Nuclear Recoil (NR), typical of α 's or neutrons. Since WIMPs are supposed to scatter producing a NR, the PSD is very helpful in decreasing the level of background in the detector. In fact, S1 is produced by a de-excitation of Ar from either singlet or triplet state, which have different decay times. The first one decays in $\sim 6 \text{ ns}$ while the second one in $\sim 1500 \text{ ns}$, the ratio to singlet and triplet state differs for NR and ER and this represents, definitely, the cornerstone of the PSD. This potentiality is used through a parameter called f_{90} , defined as the fraction of S1 accumulated within the first 90 ns. Regarding the calibration of the system [3], it has been done using neutron and gamma sources and $^{83\text{m}}\text{Kr}$ injected from outside and exploiting the presence of the ^{37}Ar isotope into the total amount of LAr. To obtain the best calibration of the response of S1 and S2 for nuclear recoils needed for the DarkSide program, members of the collaboration and others performed an experiment, called SCENE, that measured the intrinsic scintillation and ionization yield of recoiling nuclei in liquid argon as a function of applied electric field by exposing a small LAr TPC

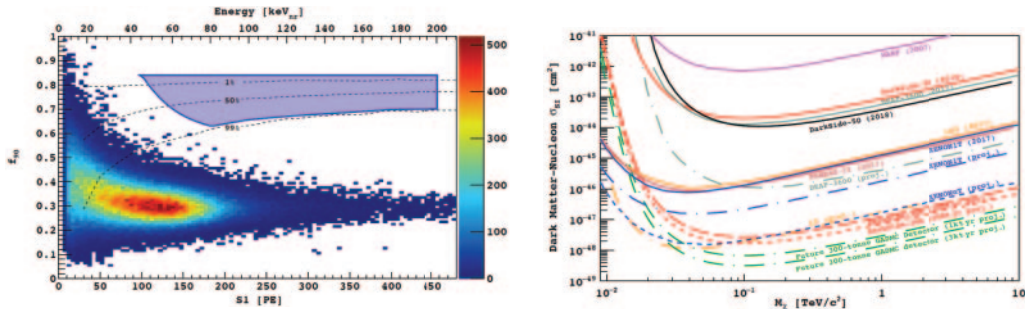


Fig. 2. – On the left, the WIMP search box in the $S1$ vs. f_{90} region after all the cuts is shown. On the right, the black curve represents the DarkSide-50 90% CL limit on the spin-independent cross-section between WIMP and nucleons.

to a low-energy pulsed narrowband neutron beam [4]. The S1 PhotoElectron (PE) yield at the TPC center was measured at 7.0 ± 0.3 PE/keV with 200 V/cm drift field and at the ^{83m}Kr peak energy of 41.5 keV. The amplification factor for the ionization signal is equal to 23 ± 1 PE per electron extracted in the gas phase with a resolution of about 20%.

3. – High-mass WIMP analysis

The analysis of DarkSide-50 in the high mass range was performed in a blind-mode on the 532.4 live-day data set [5]. This means that candidate selection/background rejection was designed, and the background surviving cuts was estimated, without knowledge of the number or properties of events in the final search region. The data are reported in the f_{90} vs. $S1$ region (fig. 2). During the analysis, the first operation consisted in opening sections of the blinded data outside of the WIMP search region to provide samples enriched in particular backgrounds for study, and later, when the background predictions would be mature, to test the predictions. The expected background was classified into three categories: surface events, neutrons (cosmogenic and radiogenic), and ERs. The number of surviving events expected using the entire statistics and after all the background rejection is 0.09 ± 0.04 , while the total acceptance after the cuts has become $72.5 \pm 0.1(\text{stat}) \pm_{0.4}^{0.5}(\text{syst})$, whose impact is accounted for in considering the fiducial mass as (31.3 ± 0.5) kg. After data unblinding, no events were observed in the defined WIMP search region, as shown in fig. 2. The lack of observed events is consistent with up to the 2.3 WIMP-nucleon scattering expected at 90% CL, which sets an upper limit on the spin-independent scattering cross-section corresponding to $1.14 \times 10^{44} \text{ cm}^2$ ($3.79 \times 10^{44} \text{ cm}^2$, $1.10 \times 10^{44} \text{ cm}^2$) for a WIMP mass of $100 \text{ GeV}/c^2$ ($1 \text{ TeV}/c^2$, $126 \text{ GeV}/c^2$), represented by the black curve shown in fig. 2. The limit is calculated assuming the standard halo model and using $v_{\text{esc}} = 544 \text{ km/s}$, $v_0 = 220 \text{ km/s}$, $v_{\text{Earth}} = 232 \text{ km/s}$, and $\rho_{\text{DM}} = 0.3 \text{ GeV}/c^2 \text{ cm}^3$.

4. – Low-mass WIMP analysis

The very important achievement reached by DarkSide consists in the background-free condition in the high-mass regime. However, relaxing the background-free requirement, it is possible to exploit the DarkSide-50 detector to perform analysis for lower energies,

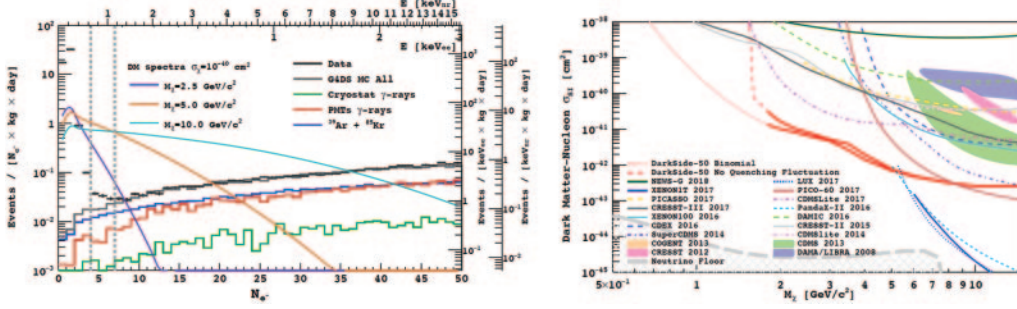


Fig. 3. – On the left, the number of events after cuts as a function of the number of ionisation electrons. On the top of the plot, the energy scale is also shown. On the right, the red curves represent the DarkSide-50 90% CL limit on the spin-independent cross-section between low-mass WIMP and nucleons under two hypotheses of quenching behaviour.

associated to the search for lower masses of WIMPs [6]. In order to decrease the threshold only the S2 signal was used. On the other hand, not considering S1 means that PSD is therefore not available. The efficiency of the software pulse finding algorithm is essentially 100% for S2 signals larger than 30 PE. The energy threshold for this analysis was set at $4e^-$, which corresponds to ~ 92 PE. Since S1 is not exploitable, neither the z -fiducialization is available. Moreover, at low energies the low statistics does not allow to use the xy algorithm for the radial fiducialization, thus the choice was to define a fiducial region only accepting events where the largest S2 signal is recorded in one of the seven central top-array PMTs. This means that the detector acceptance for this analysis is 0.42 ± 0.01 , reducing the fiducial mass. The ionisation yield has been determined using *in situ* calibration data from $^{241}\text{Am}^{13}\text{C}$ and $^{241}\text{AmBe}$ neutron sources, combined with the data from SCENE and ARIS [7]. The events collected during the live-time of the detector and after the cuts are shown in fig. 3. Precisely, three different ranges are defined. The first one is above $7 e^-$, where the observed rate of events ($\sim 1.5/\text{keV}_{ee} \text{ day kg}$) is very well reproduced by the Monte Carlo simulation used. This consistence validates the simulation in the range above 0.6 keV_{ee} . The second region to be considered is between 4 and $7 e^-$, where there is small excess of events with respect to the Monte Carlo predictions, which is not understood and left for further studies. Finally, in the region below $4 e^-$ a huge excess of events is observed. However, these are observed to be correlated in space and time with preceding events with large ionization, thus they are believed to be electrons trapped and subsequently released by impurities. Setting the threshold at $4 e^-$, the low-energy excess is not taken into account, while the intermediate small excess limits the sensitivity in the WIMP mass region between $1.8 \text{ GeV}/c^2$ and $3 \text{ GeV}/c^2$. The uncertainty on the expected WIMP signal near the threshold is dominated by the average ionization yield, as extracted from calibrations, and its intrinsic fluctuations, modelled by applying binomial statistics to the ionization yield and the recombination processes. Upper limits on the WIMP-nucleon scattering cross-section are extracted from the observed e spectrum using a binned profile likelihood method. Nowadays, this is the strongest limit obtained by a dark matter detector in the low-mass region. Improved ionization yield measurement and assessment of a realistic ionization fluctuation model, which are left for future work, may be used to determine the actual sensitivity of the present experiment within the range indicated.

5. – Sub-GeV dark-matter–electron analysis

Nowadays, since the phase space available for the different WIMP models has been significantly constrained by the very precise limits set by the different experiments, physicists are led to exploring new possibilities for dark matter. One of those is in the dark-sector framework, predicting sub-GeV particles with smaller coupling with respect to the weak scale. For these models, a new mediator boson is assumed and depending on its unknown mass, the predictions of the expected rate of events are different. In this analysis two opposite limits are discussed, very heavy and very light mediator [8]. Sub-GeV particles cannot be detected by the effects of the elastic nuclear recoils, since their kinetic energy is too small. However, if dark matter scatters directly on the bound electrons of the target, the kinematics is more favorable and is sufficient to ionize the target atom and to produce a visible signal in detectors. The interaction induces an ER signal, whose response is therefore not subjected to the quenching uncertainty of the ionization signal induced by WIMP-nucleus interactions. Searching for these DM-electron interactions requires the same data selection described for the low-mass WIMP analysis but with a threshold set to $3 e^-$, equivalent to 0.05 keV_{ee} . A very important goal regarding the energy calibration is achieved exploiting the presence of the ^{37}Ar isotope. Indeed, this disintegrates by 100% electron capture transition to the nuclear ground state of the ^{37}Cl nuclide. The recommended value for the ^{37}Ar half-life is 35.01 ± 0.02 days. The lines coming from the L-shell have an energy of 0.27 keV , while those from the K-shell have an energy of about 2.81 keV and most of those ($>90\%$) are produced by Auger electrons. DarkSide-50 observed that the sample of ^{37}Ar was almost completely decayed after 100 days. The resulting ionization spectra, shown in fig. 4, are then smeared considering

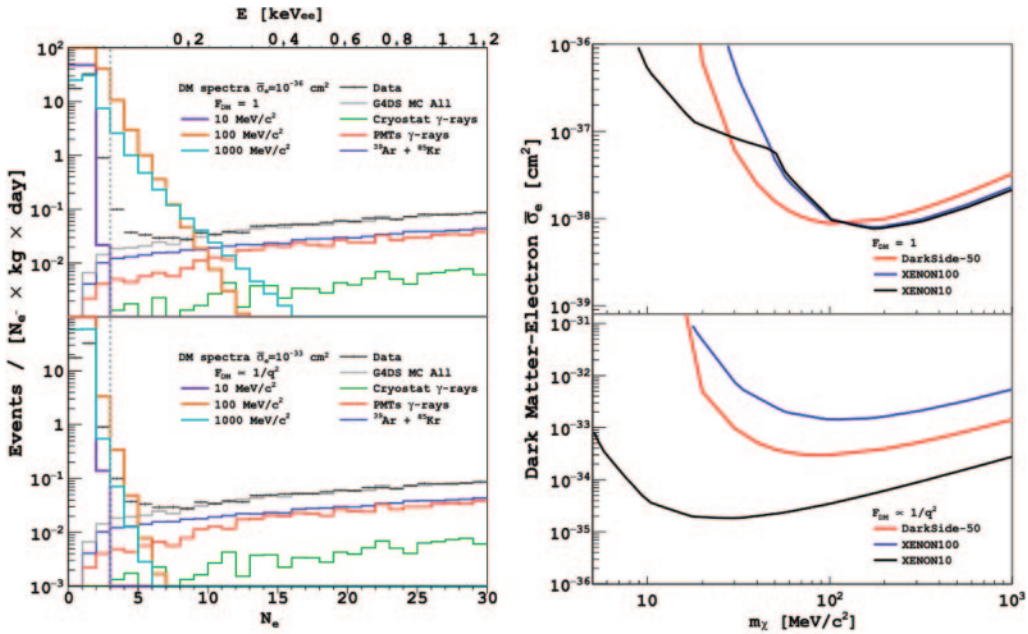


Fig. 4. – On the left, the number of events obtained with the S2-only analysis compared with the spectra for the interaction DM-electron. On the right, the DarkSide-50 90% CL limit in two different regimes: heavy mediator, on top, and light mediator, on bottom.

the ionization yield and recombination processes and convolving them with the detector response, measured from single-electron events. The resulting 90% CL limits are shown in fig. 4 for two different mediator assumptions. In the case of a light mediator, the constraints from DarkSide-50 are not as stringent as those from XENON10, while in the heavy-mediator regime this constraints improve the existing limits from XENON10 and XENON100, for dark matter masses between $30 \text{ MeV}/c^2$ and $100 \text{ MeV}/c^2$, seeing a factor-of-3 improvement at $50 \text{ MeV}/c^2$.

6. – Conclusion

In this contribution the latest results obtained from the analysis of 532.4 days of data collected with the DarkSide-50 detector have been discussed. In the high-mass search, DarkSide-50 has demonstrated to be able to achieve a zero-background regime with margins for further suppression. The results obtained are extremely promising and set the basis for future detectors, called DarkSide-20k [9] and ARGO, which will provide a multi-tonne argon target mass capable of collecting an exposure of hundreds tonne year. Finally, exclusion limits at low-mass WIMPs and sub-GeV particles have been presented.

REFERENCES

- [1] DARKSIDE COLLABORATION (AGNES P. *et al.*), *Phys. Lett. B*, **743** (2015) 456.
- [2] DARKSIDE COLLABORATION (AGNES P. *et al.*), *JINST*, **11** (2016) 03016.
- [3] DARKSIDE COLLABORATION (AGNES P. *et al.*), *JINST*, **12** (2017) T12004.
- [4] SCENE COLLABORATION (CAO H. *et al.*), *Phys. Rev. D*, **91** (2015) 092007.
- [5] DARKSIDE COLLABORATION (AGNES P. *et al.*), *Phys. Rev. D*, **98** (2018) 102006.
- [6] DARKSIDE COLLABORATION (AGNES P. *et al.*), *Phys. Rev. Lett.*, **121** (2018) 081307.
- [7] ARIS COLLABORATION (AGNES P. *et al.*), arXiv:1801.06653 (2018).
- [8] DARKSIDE COLLABORATION (AGNES P. *et al.*), *Phys. Rev. Lett.*, **121** (2018) 111303.
- [9] DARKSIDE COLLABORATION (AGNES P. *et al.*), *Eur. Phys. J. Plus*, **133** (2018) 131.